American Journal of Engineering and Applied Sciences

Original Research Paper

Spinel $NiCo_2O_4$ Nanorods for Supercapacitor Applications

Surjit Sahoo, Satyajit Ratha and Chandra Sekhar Rout

School of Basic Sciences, Indian Institute of Technology, Bhubaneswar, 751013, India

Article history
Received: 07-04-2015
Revised: 01-05-2015
Accepted: 29-05-2015

Corresponding Author:
Chandra Sekhar Rout
School of Basic Sciences, Indian Institute of Technology,
Bhubaneswar, 751013, India
Email: csrout@iitbbs.ac.in

Abstract: Herein, we report successful synthesis method of spinel $NiCo_2O_4$ nanorods by a low-cost and facile hydrothermal route. Cyclic Voltametry (CV) and galvanostatic Charge-Discharge (CD) measurements deduce ideal supercapacitive performance (823 F/g) of spinel $NiCo_2O_4$ nanorods at a nominal current density of 0.823 A/g with excellent cyclic stability and energy density of 28.51 Wh/Kg.

Keywords: $NiCo_2O_4$, Ternary Metal Oxide, Nanorods, Energy Storage, Supercapacitor

Introduction

Advancement of science, technology and rapid industrial progress in the 21st century have already played a pivotal role in causing some serious environment related issues like pollution, global warming, climate change and scarcity of fossil fuels and other non-renewable energy sources. Also the huge demand for energy and power has further complicated the situation. There is an urgent requirement for more cleaner and environment friendly alternate energy resources/devices which could possibly meet up to the expected energy demand, globally and will have negligible/zero contribution towards environment related pollution issues (Dubal *et al*., 2015; Garg *et al*., 2014). As alternative energy conversion/storage options, solar cells, (Green *et al*., 2015) fuel cells, (Galeano *et al*., 2014; Dusastre 2013; Kafafi, 2015) supercapacitors (Jokar *et al*., 2015; Lu *et al*., 2013) have exhibited profound attention in recent years. Supercapacitors are an emerging energy storage option having the combined property of both capacitor and battery. For an energy storage device, it is highly expected that there should be no time lag during charging (similar to a typical capacitor) and also the self-discharge should be much lower (as in case of a typical electrochemical battery) which would result in a higher power density and energy density, respectively. Therefore supercapacitors possess this unique hybrid property of being able to charge within a very short time period and keep it as long as possible without any significant loss. With the rapid growth in areas like portable electronics with light weight and flexible designs, research on these storage devices is of immense significance. The key research on supercapacitor is to enhance the specific capacitance as well as energy density (Garg *et al*., 2014; Miller and Simon, 2008; Simon and Gogotsi, 2008). Hybrid supercapacitors show both electrochemical double layer capacitance (EDLC) and pseudocapacitance (due to reversible faradaic redox reaction) because EDLC alone is not enough to deliver sufficient amount of energy/power (Lu *et al*., 2013; Jokar *et al*., 2015). Also pseudocapacitance is much higher as compared to EDLC. So for practical applications, requirement of better pseudocapacitive materials is obvious.

Recently, there has been growing interest in nanostructured materials with specific morphology like three dimensional (3D) urchins, (Wang *et al*., 2012b) two dimensional (2D) nanosheets (Zhang and Lou, 2013) and one dimensional (1D) nanoneedles, (Zhang *et al*., 2012) nanowires (Zhu *et al*., 2013) and nanorods (Salunkhe *et al*., 2011) for their possible application as supercapacitor electrodes due to their enhanced electrochemical properties, high specific surface area and availability of short electron and ion transport pathways (Zou *et al*., 2013). Two dimensional transition metal oxides (TMOs) like RuO_2, (Zang *et al*., 2008) Co_3O_4, (Xia *et al*., 2011) NiO (Zhang *et al*., 2010) and Mn_3O_4 (Dubal *et al*., 2009) have been widely studied as electrodes for supercapacitors. Among all, RuO_2 has been considered as an influential material because of its high specific capacitance and much better cyclic stability (Bi *et al*., 2010). But the high cost and toxicity associated with it makes its commercialization improbable (Lu *et al*., 2012; Zhao *et al*., 2009; Ghodbane *et al*., 2009). Several attempts have been made to find other alternate cost-effective, non-toxic, environment friendly electrode materials. Among all, oxides of first row transition-metals like Mn, Fe, Co, Ni etc. have shown promising results as active materials suitable for supercapacitor electrodes. Oxides of both cobalt and nickel have shown unique electrochemical behavior owing to the high redox activity of their respective metal ions (Ghosh *et al*., 2014; Yuan *et al*., 2009). Mixed transition metal oxides (MTMOs), typically ternary metal oxides with two different metal cations have got large attention in recent years due to their spectacular roles in many energy related applications (Dubal *et al*., 2015). Many spinel oxides fall into this category having a compositional formula of AB_2X_4, in which A and B are two different transition metals such as Fe, Ni, Co, Mn, Zn etc (Dubal *et al*., 2015). Among different MTMOs, nickel cobalt oxide ($NiCo_2O_4$) is currently emerging as one of the most intriguing material in the field of super capacitors (Dubal *et al*., 2015). It belongs to the group of normal spinels similar to $MgAl_2O_4$, $ZnCr_2O_4$, $ZnAl_2O_4$ and $ZnCo_2O_4$ etc., (Ratha *et al*., 2015) and has a space symmetry group $Fd\overline{3}m \equiv O_h^7$ (Garg *et al*., 2014). Ternary nickel cobalt oxide ($NiCo_2O_4$) is inexpensive, non-toxic, eco-friendly and has different morphologies with impressive supercapacitive properties compared to its binary metal oxides counterparts (Dubal *et al*., 2015). In this report, synthesis, characterization and detailed electrochemical studies of 1D nickel cobalt oxide (NCO) nanorod arrays have been described. Electrochemical measurements showed that the nickel cobalt oxide electrodes do exhibit better specific capacitance of ~823 Fg^{-1} at a current density of 0.823 Ag^{-1} and ~470 Fg^{-1} at a scan rate of 4 mV/s and possesses a good energy density of the order of 28.51 Wh/Kg.

Experimental Section

Chemicals

Nickel nitrate hexahydrate [$Ni(NO_3)_2.6H_2O$, 98%, Merck Specialties private limited (India)], Cobalt nitrate hexahydrate [$Co(NO_3)_2.6H_2O$, 97%, Merck Specialties private limited (India)], Urea [CH_4N_2O, 99.5%, Sisco Research Laboratories private limited (India)] were used to synthesize $NiCo_2O_4$ nanorods. For electrochemical measurements, 2M aqueous solution of potassium hydroxide [KOH, 85%, Alfa Aesar (UK)] was used. All the above chemicals were of analytical grade and used as received without further modification.

Synthesis Procedure for $NiCo_2O_4$ Nanorods

Figure 1 shows the schematic elucidating different phases of growth for the NCO nanorods. The $NiCo_2O_4$ nanorods were synthesized by a simple hydrothermal method. In a typical process, $Ni(NO_3)_2.6H_2O$ (3 mmol), $Co(NO_3)_2.6H_2O$ (6 mmol) and urea (60 mmol) were first dissolved in 40 mL of DI water and then the solution was ultrasonicated for 15 min at room temperature. The resulting mixture was transferred to a 50 mL Teflon lined stainless steel autoclave, which was heated at 90°C for 12 h . in a hot air oven. In aqueous solution, urea has a tendency to get hydrolyzed forming Co_3^{2-} and OH-ions. When nickel precursor and cobalt precursor are dissolved in above aqueous solution containing urea, nickel ions and cobalt ions get nucleated in the presence of urea to form self-assembled growth patterns (Xiao and Yang, 2011; Ratha *et al*., 2015). Similar synthesis procedure was carried out at different temperatures, i.e., 90°C, 120°C, 150°C and180°C. After the hydrothermal reaction for 12 h, the autoclaves were allowed to cool naturally to room temperature. The precipitates were collected by centrifugation and then dried at 100°C for 4 h and was further annealed at 200°C for 6 h in a vacuum oven. The $NiCo_2O_4$ samples prepared at 90°C, 120°C, 150°C and 180°C are being labeled as NCO-90, NCO-120, NCO-150, NCO-180 and NCO-200 respectively.

Characterization

All the $NiCo_2O_4$ samples were characterized by FESEM (MERLIN Compact with GEMINI I electron column, Zeiss Pvt. Ltd., Germany) and by elemental mapping with EDAX. X-Ray Diffraction (XRD) patterns of the samples were obtained by a Bruker D8 Advanced diffractometer using Cu-Kα radiation (λ = 1.54184 A°).

Electrode Fabrication

First the surface of a bare glassy carbon electrode (GCE) was sequentially polished with micro polishing powder (Al_2O_3 powder having different grain sizes such as 1.0 µm, 0.3 µm and 0.05 µm) to get a mirror finish and it was subsequently sonicated with DI water for about 15 min in order to remove any adsorbed species on the electrode surface. About 1mg of the as synthesized sample was dispersed in a mixture of 95 µL of ethanol and 5 µL of nafion which was further ultrasonicated for 10 min to give a homogeneous mixture solution. Then 2.5 µL of the mixture solution was drop casted on to the surface of the freshly polished glassy carbon electrode and then it was dried in a vacuum desiccator for 1 h. By comparing the weight of the glassy carbon electrode before sample loading and after sample loading, the mass of the sample deposited on the GCE surface was found to be 0.034 mg.

Electrochemical Measurements

The electrochemical performance of the $NiCo_2O_4$ nanorods modified electrode was evaluated in a three electrode electrochemical cell using a Potentiostat/Galvanostat (PG-16125, Techno science instrument, Bangalore, India) in 2 M aqueous solution of KOH working as the electrolyte. A basic schematic of the three electrode cell arrangement is shown Fig. 2. The CV and CD measurments were carried out at room temperature at different scan rates and different current densities keeping the potential window between -0.1V to 0.4V Vs. Ag/AgCl electrode. The specific/gravimetric

Capacitance (C_{sp}) was calculated from cyclic voltammetry curves using the following Equation 1:

$$C_{sp} = \frac{\int_{-0.1}^{0.4} I(V)dV}{m.s\left[V_f - V_i\right]} \quad (1)$$

where, the integral part in the numerator gives the area under the CV curve, m is the mass of the sample loaded onto the GCE surface, s is the scan rate and $[V_f\text{-}V_i]$ is the potential window (V_f and V_i are the final and initial potential values, respectively). From charge-discharge curves, the specific capacitance of the material was calculated using the following Equation 2:

$$C_{sp} = \frac{I}{m\left(\frac{dV}{dt}\right)} \quad (2)$$

where, I is the discharge current, m is the mass of the sample loaded onto the GCE surface and dV/dt is the slope of the discharge curve. To calculate the Energy density (E_d) and Power density (P_d) for the sample, following Equation 3 and 4 were used:

$$E_d = \frac{1}{2} C_{sp} V^2 \quad (3)$$

$$P_d = \frac{1}{2} C_{sp} V.s \quad (4)$$

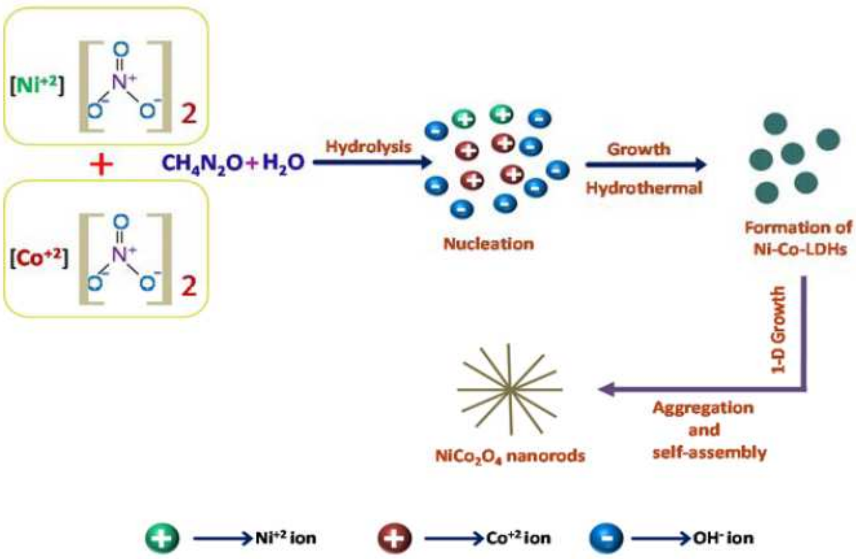

Fig. 1. Schematic showing an illustrative representation of synthesis procedure and growth mechanism of $NiCo_2O_4$nanorods

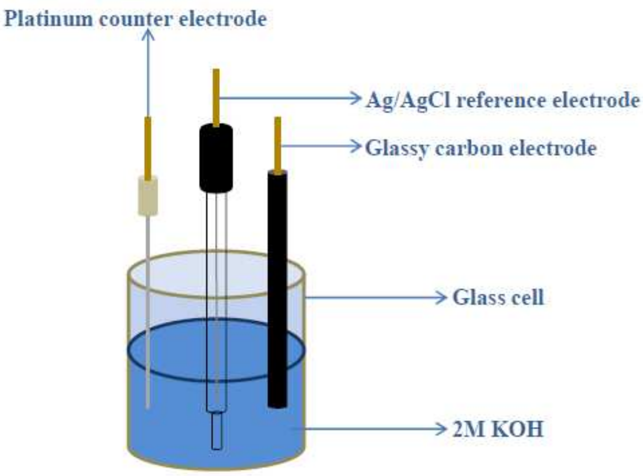

Fig. 2 Schematic showing a typical three-electrode cell configuration used for the electrochemical measurements

Results and Discussion

Morphological Study

Figure 3 shows the FESEM images of the samples prepared at different temperatures in which the formation of nanorod shaped NCO is clearly depicted. Similarly, Fig. 4a and b show the FESEM images of the sample prepared at 200°C which confirms the formation of nanorod like NCO. On an average, these nanorods are having a diameter of 50-60 nm and a length in the range of ~0.2-1 μm. The EDAX spectrum and elemental composition data is shown in Fig. 4c. Elemental analysis show the Ni and Co ratio of ~1:2, confirming formation of $NiCo_2O_4$ phase. Figure 5 shows the elemental mapping data for the NCO-200 sample. In Fig. 6, X-ray diffraction patterns of NCO samples prepared at different temperatures have been shown. From the XRD patterns, it is confirmed that the sample synthesized at 200°C is of high crystallinity compared to the samples prepared at lower temperatures. All the diffraction peaks match with JCPDS file No. 20-0781 and showed a prominent growth along (311) direction. All the peaks can be assigned to a face centered cubic lattice of spinel NCO.

Supercapacitive Study

We performed systematic electrochemical supercapacitor measurements of NCO-200 due to its high crystallinity compared to the NCO prepared at lower temperatures. Systematic electrochemical measurements such as CV and CD were performed in presence of 2 M KOH as electrolyte. For cyclic voltammetry and charge discharge measurments, the potential window was kept within the range -0.1 to 0.4 V. Figure 7a shows the cyclic voltammogram curves of NCO-200 at different scan rates. From Fig. 7d it is observed that the specific capacitance decreases gradually with increase in scan rate. Also from Fig. 7a, it can be inferred that with increase in scan rate, the anodic peak shifts towards positive potential and the cathodic peak shifts towards negative potential. From the specific capacitance calculation from CV curves, the maximum value of specific Capacitance (C_{sp}) was found to be 470.58 F/g at 4 mV/s. Similarly, to further quantify the specific Capacitance (C_{sp}) of NCO-200, galvanostatic charge-discharge experiments were conducted in the three electrode cell configuration at various current densities with the same potential window between -0.1 to 0.4V. Figure 7b shows the charge discharge curves of NCO-200 at different current densities. Specific capacitance (C_{sp}) of values 823 F/g, 460 F/g and 382 F/g were obtained at current densities of 0.8 A/g, 1.38 A/g, 3.44 A/g and 5.58 A/g, respectively. Similarly from Fig. 7c, it is observed that with increase in current density, the specific capacitance decreases gradually.

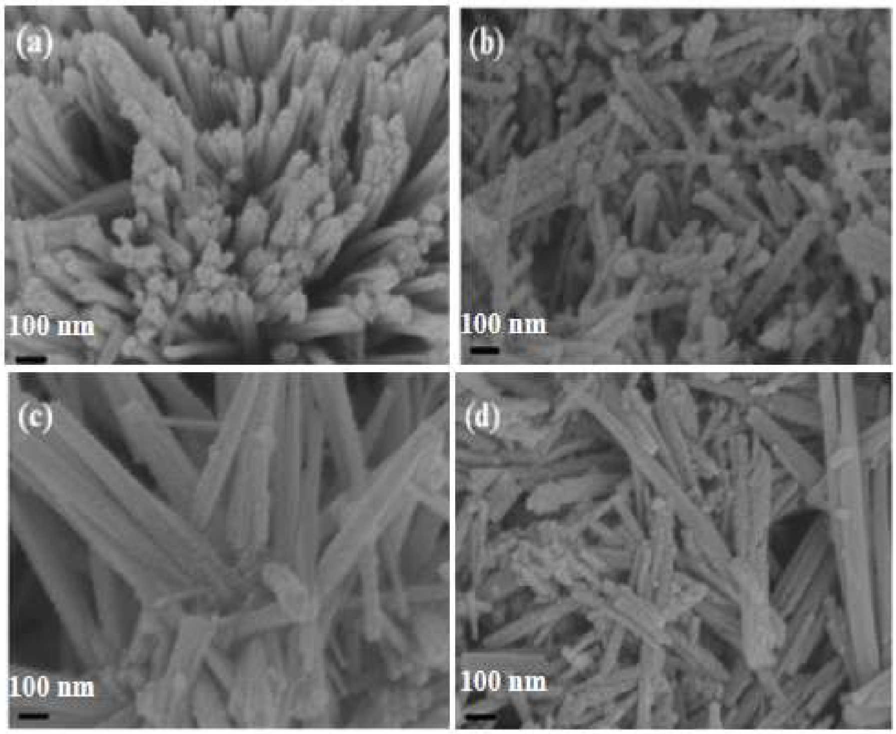

Fig. 3. FESEM images of (a) NCO-90 (b) NCO-120 (c) NCO-150 and (d) NCO-180

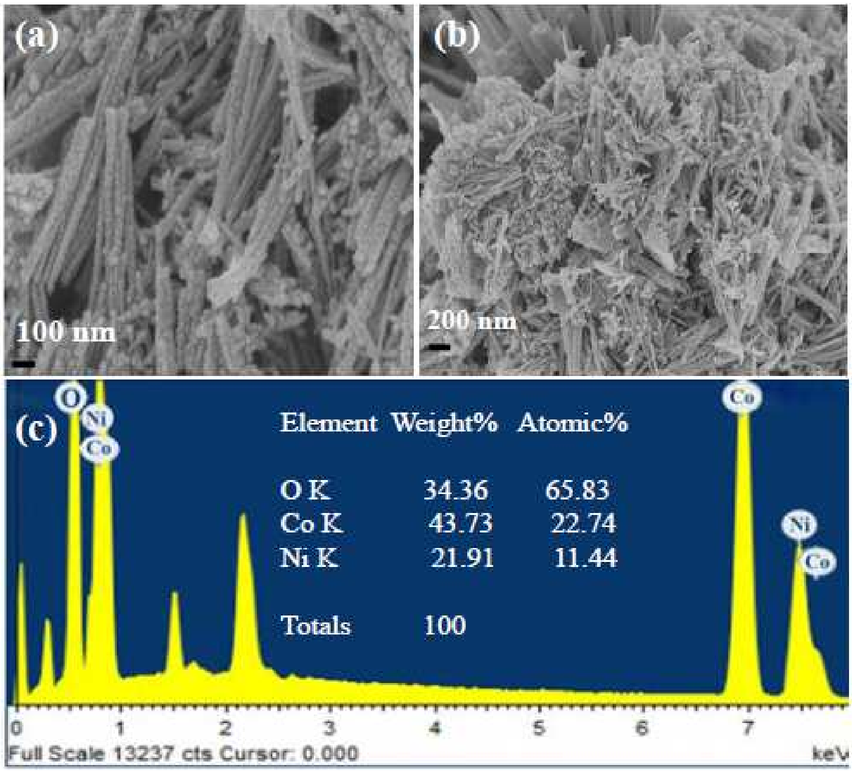

Fig. 4. (a), (b) FESEM images of NCO-200 and (c) EDS spectra with inset showing percentage of composition of constituent elements (Ni,Co,O)

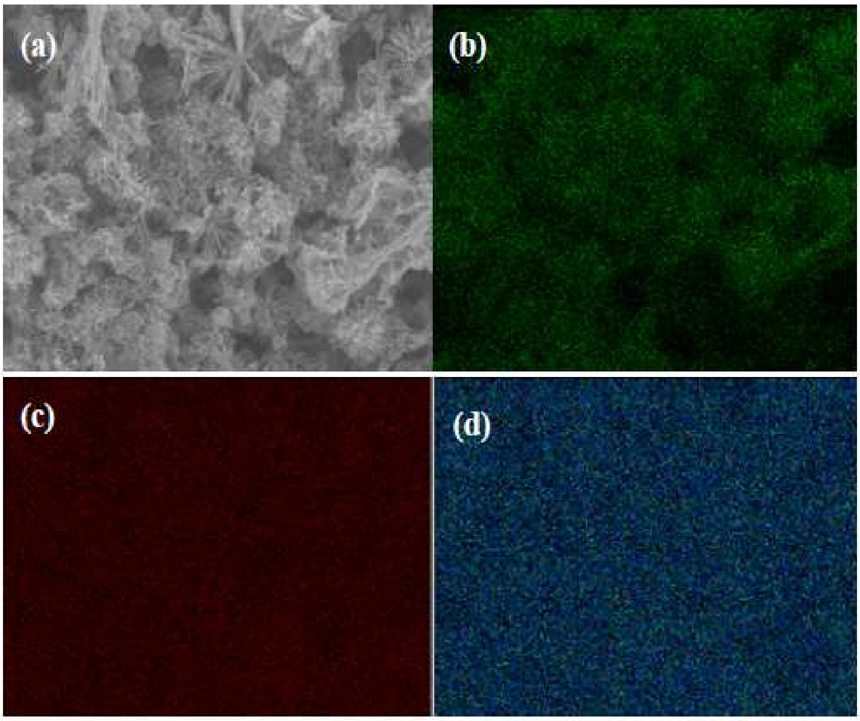

Fig. 5. Elemental mapping of NCO-200 (a) electronic image over which mapping has been performed, presence of oxygen (b) cobalt (c) and nickel (d) is confirmed from the mapping data

DOI: 10.3844/ajeassp.2015.371.379

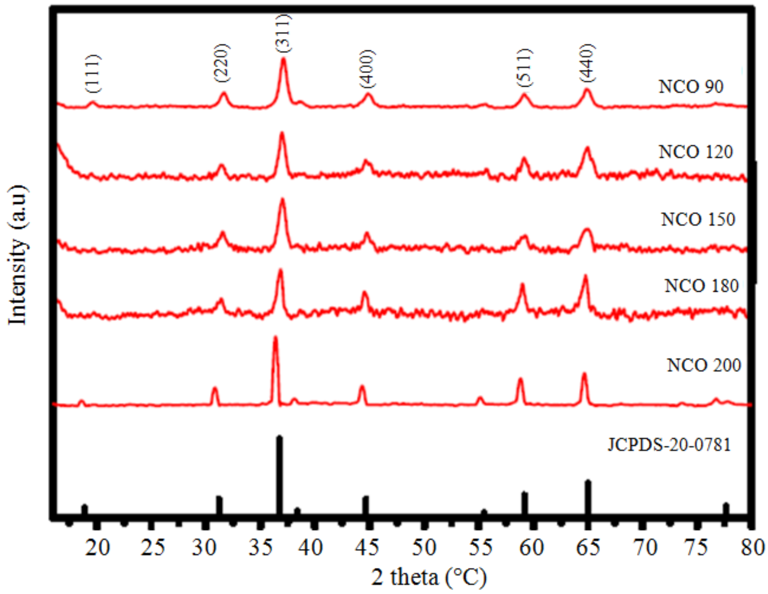

Fig. 6. X-ray diffraction patterns of NCO samples prepared at different temperatures and comparison with JCPDS file No. 20-0781 of $NiCo_2O_4$

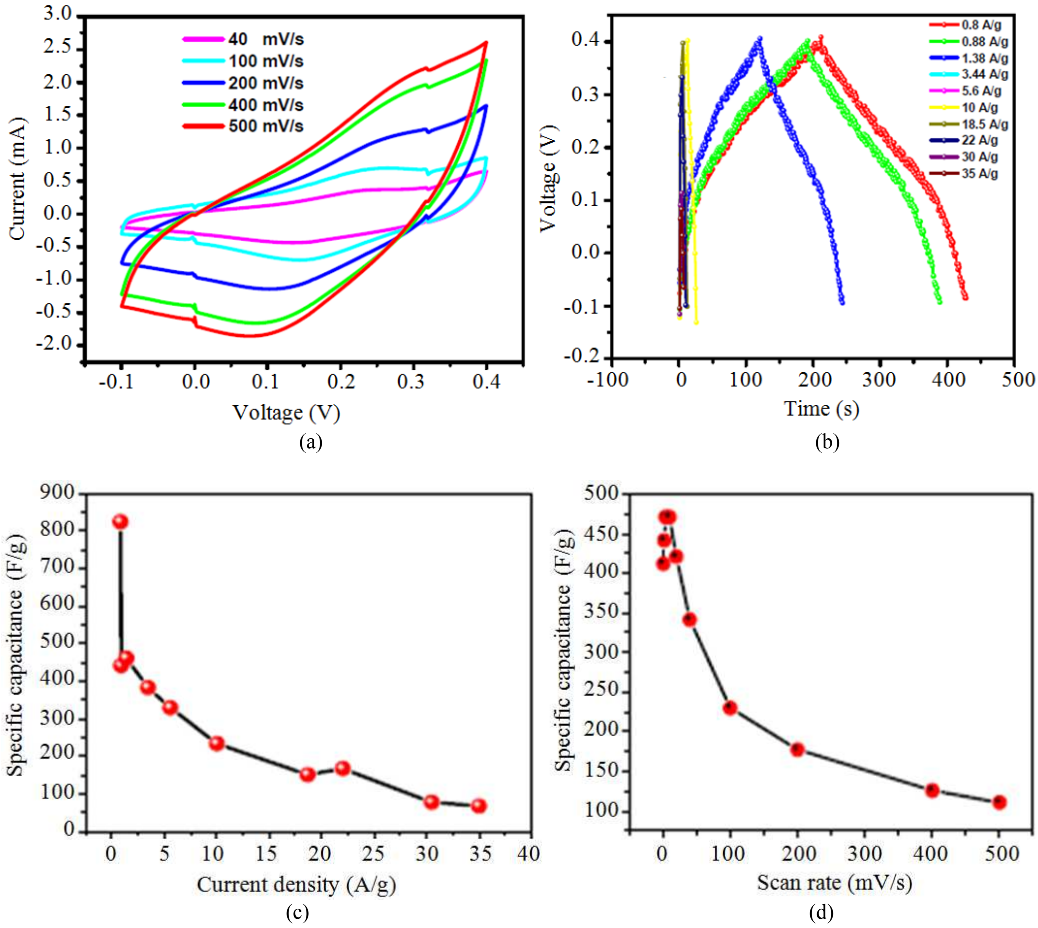

Fig. 7. Electrochemical study of NCO-200 (a) Cyclic voltammetry curves at different scan rates (b) charge-discharge curves obtained at different current densities variation of obtained specific capacitance with respect to (c) current density and (d) scan rates

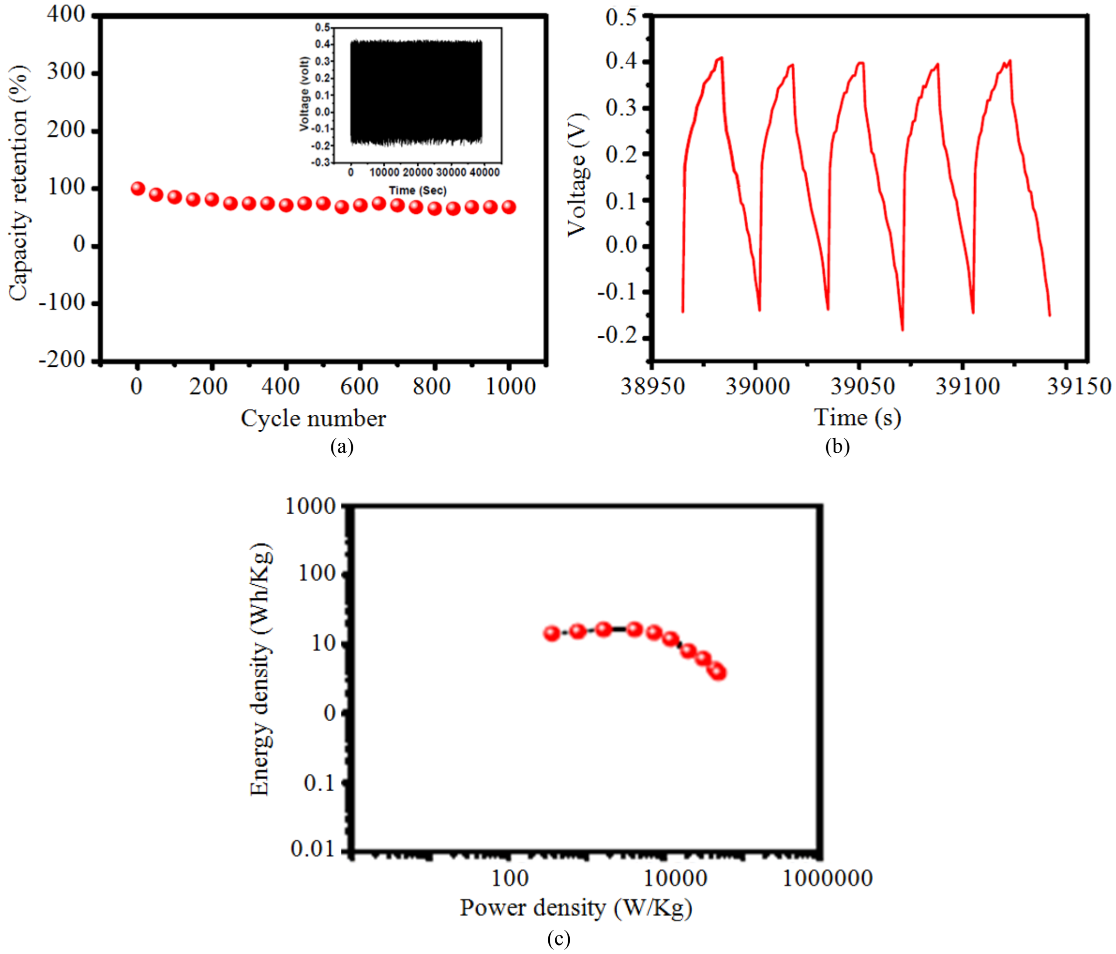

Fig. 8. (a) Cycle number vs. percentage of capacity retention of the NCO-200 showing good stability over 1000 cycles(inset shows CD curves of 1000 cycles) (b) Curves of last five cycles, (c) Ragone plot showing the dependence of energy density and power density

A long cycling stability performance of any material is the most important criteria for its possible application as supercapacitor electrode (Wang *et al*., 2012a; 2010). Figure 8a shows the capacitance retention capability of NCO-200 over 1000 cycles with the inset showing 1000 charge-discharge curves. The galvanostatic charge discharge was performed for 1000 cycles at a current density of 5.58 A/g. The sample shows excellent cycling stability which is evident from the fact that even after 1000 cycles, the retention of supercapacitor performance remained close to the initial value which is shown in Fig. 8a. Similarly Fig. 8b shows the charge-discharge curve of last 5 cycles of 1000 cycles. The Ragone plot showing the relationship between energy density and power density has been shown in Fig. 8c. The maximum energy density and power density from the graph was found to be 28.51 Wh/Kg and 49.9 KW/Kg respectively. The specific capacitance for NCO-200 was found to be 823 F/g at current density of 0.8 A/g which is very much comparable to previously reported values. Tang *et al*. (2013) have shown that NCO nanowires exhibit a specific capacitance of 760 F/g at a current density of 1 A/g. Similarly, urchin shaped $NiCo_2O_4$ in sequential crystallization process shows a specific capacitance, 658 F/g at 1 A/g synthesized by Wang *et al*. (2012). Deng *et al*. (2014) have synthesized $NiCo_2O_4$ nanowires on carbon fiber paper via solvothermal method with specific capacitance, 690 F/g at a current density of 16 A/g. Pu *et al*. (2013) have synthesized $NiCo_2O_4$ nanoplates via hydrothermal method shows specific capacitance 294 F/g at current density of 1 A/g. The NCO-200, reported here shows supercapacitive behavior which is very much comparable to the above reported values and has a potential to be used as a supercapacitor electrode for next generation energy storage devices.

Conclusion

In summary, $NiCo_2O_4$ nanorods were synthesized by a facile hydrothermal route at different temperatures i.e., 90°C, 120°C, 150°C, 180°C and 200°C. The growth mechanism of the NCO nanorods were discussed and its supercapcitor performance was tested in a 3- electrode configuration in 2M aqueous KOH solution. The supercapacitive properties of $NiCo_2O_4$ synthesized at 200°C were studied in detail. The specific capacitance (C_{sp}) of the NCO-200 reached as high as 823 Fg^{-1} at a current density of 0.823 Ag^{-1} with energy density of 28.51 Wh/Kg and also showed excellent cyclic stability even after 1000 charge-discharge cycles. So these results readily explain the viable application of spinel $NiCo_2O_4$ nanorods as high performance electrode material for supercapacitor application.

Funding Information

Dr. C.S. Rout would like to thank DST (Government of India) for the Ramanujan fellowship. This work was supported by the BRNS-DAE, Government of India (Grant No. 37(3)/14/48/2014-BRNS/1502).

Author's Contributions

All authors equally contributed in this work.

Ethics

The authors declare no competing financial interest.

References

Bi, R.R., X.L. Wu, F.F. Cao, L.Y. Jiang and Y.G. Guo *et al*., 2010. Highly dispersed RuO_2 nanoparticles on carbon nanotubes: Facile synthesis and enhanced supercapacitance performance. J. Phys. Chem. C, 114: 2448-51. DOI: 10.1021/jp9116563

Deng, F., L. Yu, M. Sun, T. Lin and G. Cheng *et al*., 2014. Controllable growth of hierarchical $NiCo_2O_4$ nanowires and nanosheets on carbon fiber paper and their morphology-dependent pseudocapacitive performances. Electrochimica Acta, 133: 382-90. DOI: 10.1016/j.electacta.2014.04.070

Dubal, D.P., D.S. Dhawale, R.R. Salunkhe, S.M. Pawar and V.J. Fulari *et al*., 2009. A novel chemical synthesis of interlocked cubes of hausmannite Mn_3O_4 thin films for supercapacitor application. J. Alloys Compounds, 484: 218-21. DOI: 10.1016/j.jallcom.2009.03.135

Dubal, D.P., P. Gomez-Romero, B.R. Sankapal and R. Holze, 2015. Nickel cobaltite as an emerging material for supercapacitors: An overview. Nano Energy, 11: 377-99. DOI: 10.1016/j.nanoen.2014.11.013

Dusastre, V., 2013. Anhydrous polymer electrolyte. Nat. Mater., 13: 2-2. DOI: 10.1038/nmat3856

Galeano, C., C. Baldizzone, H. Bongard, B. Spliethoff and C. Weidenthaler *et al*., 2014. Carbon-based yolk-shell materials for fuel cell applications. Adv. Funct. Mater., 24: 220-32. DOI: 10.1002/adfm.201302239

Garg, N., M. Basu and A.K. Ganguli, 2014. Nickel cobaltite nanostructures with enhanced supercapacitance activity. J. Phys. Chem. C, 118: 17332-41. DOI: 10.1021/jp5039738

Ghodbane, O., J.L. Pascal and F. Favier, 2009. Microstructural effects on charge-storage properties in MnO_2-based electrochemical supercapacitors. ACS Applied Mater. Interfaces, 1: 1130-39. DOI: 10.1021/am900094e

Ghosh, D., S. Giri and C.K. Das, 2014. Hydrothermal synthesis of platelet β $Co(OH)_2$ and Co_3O_4: Smart electrode material for energy storage application. Environ. Progress Sustainable Energy, 33: 1059-64. DOI: 10.1002/ep.11874

Green, M.A., K. Emery, Y. Hishikawa, W. Warta and E. D Dunlop, 2015. Solar cell efficiency tables (version 45). Progress Photovoltaics: Res. Applic., 23: 1-9. DOI: 10.1002/pip.2573

Jokar, E., A. zad and S. Shahrokhian, 2015. Synthesis and characterization of $NiCo_2O_4$ nanorods for preparation of supercapacitor electrodes. J. Solid State Electrochem., 19: 269-74. DOI: 10.1007/s10008-014-2592-y

Kafafi, Z.H., 2015. Metal-free catalysts for fuel cell technology. Science, 347: 960-960. DOI: 10.1126/science.347.6225.960-h

Lu, Q., J.G. Chen and J.Q. Xiao, 2013. Nanostructured electrodes for high-performance pseudocapacitors. Angewandte Chemie Int. Edn., 52: 1882-89. DOI: 10.1002/anie.201203201

Lu, X., T. Zhai, X. Zhang, Y. Shen and L. Yuan *et al*., 2012. WO_{3-x}@Au@MnO_2 core-shell nanowires on carbon fabric for high-performance flexible supercapacitors. Adv. Mater., 24: 938-44. DOI: 10.1002/adma.201104113

Miller, J.R. and P. Simon, 2008. Electrochemical capacitors for energy management. Science, 321: 651-52. DOI: 10.1126/science.1158736

Pu, J., J. Wang, X. Jin, F. Cui and E. Sheng *et al*., 2013. Porous hexagonal $NiCo_2O_4$ nanoplates as electrode materials for supercapacitors. Electrochimica Acta, 106: 226-34. DOI: 10.1016/j.electacta.2013.05.092

Ratha, S., R.T. Khare, M.A. More, R. Thapa and D.J. Late *et al*., 2015. Field emission properties of spinel $ZnCo_2O_4$ microflowers. RSC Adv., 5: 5372-5378. DOI: 10.1039/C4RA10246K

Salunkhe, R.R., K. Jang, H. Yu, S. Yu and T. Ganesh *et al*., 2011. Chemical synthesis and electrochemical analysis of nickel cobaltite nanostructures for supercapacitor applications. J. Alloys Compounds, 509: 6677-82. DOI: 10.1016/j.jallcom.2011.03.136

Simon, P. and Y. Gogotsi, 2008. Materials for electrochemical capacitors. Nat. Mater., 7: 845-54. DOI: 10.1038/nmat2297

Tang, Y. and W. Cheng, 2013. Nanoparticle-modified electrode with size- and shape-dependent electrocatalytic activities. Langmuir, 29: 3125-32. DOI: 10.1021/la304616k

Wang, H., H.S. Casalongue, Y. Liang and H. Dai, 2010. $Ni(OH)_2$ nanoplates grown on graphene as advanced electrochemical pseudocapacitor materials. J. Am. Chem. Soc., 132: 7472-77. DOI: 10.1021/ja102267j

Wang, H., Y. Wang, Z. Hu and X. Wang, 2012a. Cutting and unzipping multiwalled carbon nanotubes into curved graphene nanosheets and their enhanced supercapacitor performance. ACS Applied Mater. Interfaces, 4: 6827-34. DOI: 10.1021/am302000z

Wang, Q., B. Liu, X. Wang, S. Ran and L. Wang *et al.*, 2012b. Morphology evolution of urchin-like $NiCo_2O_4$ nanostructures and their applications as psuedocapacitors and photoelectrochemical cells. J. Mater. Chem., 22: 21647-53. DOI: 10.1039/C2JM34705A

Xia, X.H., J.P. Tu, Y.J. Mai, X.L. Wang and C.D. Gu *et al.*, 2011. Self-supported hydrothermal synthesized hollow Co_3O_4 nanowire arrays with high supercapacitor capacitance. J. Mater. Chem., 21: 9319-25. DOI: 10.1039/C1JM10946D

Xiao, J. and S. Yang, 2011. Sequential crystallization of sea urchin-like bimetallic (Ni, Co) carbonate hydroxide and its morphology conserved conversion to porous $NiCo_2O_4$ spinel for pseudocapacitors. RSC Adv., 1: 588-95. DOI: 10.1039/C1RA00342A

Yuan, C., X. Zhang, L. Su, B. Gao and L. Shen, 2009. Facile synthesis and self-assembly of hierarchical porous NiO nano/micro spherical superstructures for high performance supercapacitors. J. Mater. Chem., 19: 5772-77. DOI: 10.1039/B902221J

Zang, J., S.J. Bao, C.M. Li, H. Bian and X. Cui *et al.*, 2008. Well-aligned cone-shaped nanostructure of polypyrrole/RuO_2 and its electrochemical supercapacitor. J. Phys. Chem. C, 112: 14843-47. DOI: 10.1021/jp8049558

Zhang, G. and X.W. Lou, 2013. General solution growth of mesoporous $NiCo_2O_4$ nanosheets on various conductive substrates as high-performance electrodes for supercapacitors. Adv. Mater., 25: 976-79. DOI: 10.1002/adma.201204128

Zhang, G.Q., H.B. Wu, H.E. Hoster, M.B. Chan-Park and X.W. Lou, 2012. Single-crystalline $NiCo_2O_4$ nanoneedle arrays grown on conductive substrates as binder-free electrodes for high-performance supercapacitors. Energy Environ. Sci., 5: 9453-56. DOI: 10.1039/C2EE22572G

Zhang, X., W. Shi, J. Zhu, W. Zhao and J. Ma *et al.*, 2010. Synthesis of porous NiO nanocrystals with controllable surface area and their application as supercapacitor electrodes. Nano Res., 3: 643-52. DOI: 10.1007/s12274-010-0024-6

Zhao, X., C. Johnston and P.S. Grant, 2009. A novel hybrid supercapacitor with a carbon nanotube cathode and an iron oxide/carbon nanotube composite anode. J. Mater. Chem., 19: 8755-60. DOI: 10.1039/B909779A

Zhu, W., Z. Lu, G. Zhang, X. Lei and Z. Chang *et al.*, 2013. Hierarchical $Ni_{0.25}Co_{0.75}(OH)_2$ nanoarrays for a high-performance supercapacitor electrode prepared by an in situ conversion process. J. Mater. Chem. A, 1: 8327-31. DOI: 10.1039/C3TA10790F

Zou, R., K. Xu, T. Wang, G. He and Q. Liu *et al.*, 2013. Chain-like $NiCo_2O_4$ nanowires with different exposed reactive planes for high-performance supercapacitors. J. Mater. Chem. A, 1: 8560-8566. DOI: 10.1039/c3ta11361b